

Oxygen-isotope effect of the paramagnetic-insulating to ferromagnetic-metallic transition in $\text{La}_{1-x}\text{Ca}_x\text{MnO}_3$

J. P. Franck, I. Isaac, and Weimin Chen

Department of Physics, University of Alberta, Edmonton, Alberta, Canada T6G 2J1

J. Chrzanowski and J. C. Irwin

Department of Physics, Simon Fraser University, Burnaby, British Columbia, Canada V5A 1S6

(Received 2 April 1998)

The oxygen-isotope effect of the ferromagnetic transition in $\text{La}_{1-x}\text{Ca}_x\text{MnO}_3$ was investigated from $x=20\%$ to $x=43\%$. This is the range of the conducting ferromagnetic phase. We find that $\alpha_O = -\Delta \ln T_c / \Delta \ln m$ decreases from 0.36 to 0.14 with increasing Ca concentration. A large value of $\alpha_O = 0.83$ was found for $x=20\%$, it is possibly connected with excess oxygen content. The isotope effect decreases with increasing tolerance factor, pointing to the importance of double exchange. The isotope effect at 35% Ca is independent of magnetic field. [S0163-1829(98)06833-7]

The perovskite compounds $\text{La}_{1-x}\text{Ca}_x\text{MnO}_3$ can be prepared for the complete range of Ca concentrations $0 \leq x \leq 1$ and exhibit a rich magnetic phase diagram.¹⁻³ For Ca concentrations in the range $x=20$ to $x=50\%$, the high-temperature paramagnetic phase transforms into a low-temperature metallic-ferromagnetic phase. For x in the approximate range 42 to 50%, the ferromagnetic-metallic phase transforms at lower temperatures into a charge ordered antiferromagnetic insulator.⁴ Extremely large magnetoresistance is observed near the ferromagnetic transition, due to the field dependence of the insulating to metallic transition.^{5,6} The ferromagnetic transition is considered to be due to double exchange.⁷⁻⁹ There have also been many experimental and theoretical suggestions of extremely large electron-phonon interactions in this system, these influence the transport properties, and possibly also the transition temperature.¹⁰⁻¹⁴ Jahn-Teller or magnetic polaron formation have been observed.^{15,16} Very large oxygen-isotope effects were observed for $x=10$ and 20%, and related to Jahn-Teller polaron formation.¹⁷

In the present paper we present oxygen-isotope effect studies for Ca concentrations between 20 and 43%, i.e., for the whole range of the ferromagnetic-metallic phase. The oxygen-isotope exponent α_O is defined by $\alpha_O = -\Delta \ln T_c / \Delta \ln m_O$, where T_c is the Curie temperature. The most detailed investigations were carried out at a Ca concentration of 35%. At this concentration, the magnetoresistance is largest, and the Curie temperature T_c close to its maximum value. We observed the transition magnetically at 50 G and 4 T, carried out resistance measurements in fields up to 4 T, and observed the Raman spectrum as a function of temperature from room temperature to 15 K. These investigations were carried out on sintered polycrystalline pellets. At other Ca concentrations (including another 35% Ca pair) we investigated the isotope effect on pressed powders since the use of powders facilitates the isotopic gas exchange. Here measurements of the transition were carried out magnetically at 50 G.

Samples of $\text{La}_{1-x}\text{Ca}_x\text{MnO}_3$, $x=35\%$, were prepared from stoichiometric mixtures of La_2O_3 , CaCO_3 , and MnO_2 . The mixtures were fired in air at 1100 and 1200 °C repeatedly, with regrinding between firings. A final firing in 1 atm of pure O_2 was carried out at 1200 °C, resulting in a fairly

dense pellet. This pellet was divided into two pieces, which were treated in $^{16}\text{O}_2$ or $^{18}\text{O}_2$ (1 atm) in a parallel processing system previously described.¹⁸ The pellets were gas exchanged at 950 °C (48 h), 1100 °C (48 h), and finally 1150 °C (48 h). This resulted in a ^{18}O concentration of 82% (by weight). Magnetic, resistive, and Raman studies were carried out on this pair. Back exchange with $^{16}\text{O}_2$ restored the original transition. A second comparison pair at this calcium concentration was produced by gas-exchanging powder samples at 1000 °C for 60 h. Here a 90% ^{18}O concentration was reached. Complete back exchange was possible at 950 °C (60 h). For all other concentrations, the gas exchange was carried out on powders at 950 °C for 60 h, this is sufficient for powders to achieve ^{18}O substitutions in the 90% range.

The magnetic transitions for both comparison pairs at $x=35\%$ are shown in Fig. 1. The transitions were observed after field cooling in 50 G. The transition temperature for the ^{16}O sample near 270 K agrees with the best literature values. Magnetic transition temperatures (T_c) were obtained by extrapolating the decreasing ferromagnetic part of the magnetization to zero. This procedure in general leads to a T_c less than $T_c(R_{\max})$. A downward shift of 8.2 (pellet) and 8.5 K (powder) is observed on ^{18}O substitution, this gives an oxygen-isotope exponent of 0.26 (pellet) and 0.27 (powder). No adjustment for incomplete ^{18}O substitution was applied. As seen from Fig. 1, back exchange with ^{16}O restores the original transition, both for the pellet samples and the powder samples. The magnetic transition of the pellet comparison samples were also observed in 4 T. Isotopic shifts could most easily be identified in the remanent magnetization after field cooling in 4 T. $M_{\text{rem}}=0$ is reached at 262.1 K (^{16}O), and 254.8 K (^{18}O), leading to $\Delta T_c = 7.3$ K and $\alpha_O = 0.24$.

Resistivity measurements were carried out on the 35% pellets, in fields of 0, 2, and 4 T. The resistivity shows the well-known maximum at T_c , Fig. 2. Above T_c , up to 400 K, we were able to fit the conductivity to the small polaron conduction expression of Emin and Holstein:¹⁹

$$\sigma = \sigma_0 T^{-n} \exp(-E_a/k_B T), \quad (1)$$

where $n=1$ for the adiabatic and $n=1.5$ for the nonadiabatic case.²⁰ We obtained the following values for E_a and σ_0

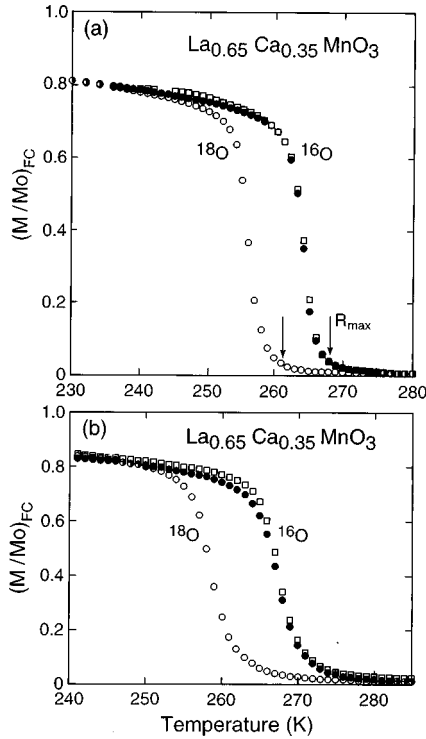


FIG. 1. Ferromagnetic transition in a field of 50 G (field cooled); black dots: ^{16}O , open circles: ^{18}O , open squares: ^{18}O samples back exchanged with ^{16}O . (a) sintered pellet samples, ^{18}O concentration 82%. The resistive maximum positions in zero field are indicated. (b) Pressed powder samples, ^{18}O concentration 90%.

(nonadiabatic values in brackets): $E_a = 89.4$ (103.0) meV for ^{16}O , $E_a = 102.6$ (117.55) meV for ^{18}O , and $\sigma_0 = 7.68 \times 10^5$ (2.25×10^7) $\Omega^{-1} \text{cm}^{-1}$ for ^{16}O , $\sigma_0 = 8.86 \times 10^5$ (3.65×10^7) $\Omega^{-1} \text{cm}^{-1}$ for ^{18}O . The ^{16}O values are in excellent agreement with data obtained by Jaime *et al.*²⁰ on a 30% Ca sputtered film.

The prefactor σ_0 is given by²⁰

$$\sigma_0 = g_d \nu_o e^2 / a k_B, \quad (2)$$

where a is an average hopping distance (Mn-Mn), ν_o a typical optical phonon frequency, and $g_d \approx 1$ depends on the

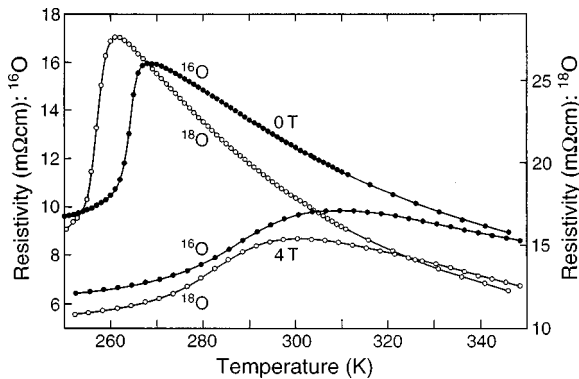


FIG. 2. Resistivity for the sintered pellet pair, $x_{\text{Ca}} = 35\%$. The isotopic shift was determined from the location of the resistive peaks. The isotope exponent α_O is essentially independent of field (see text).

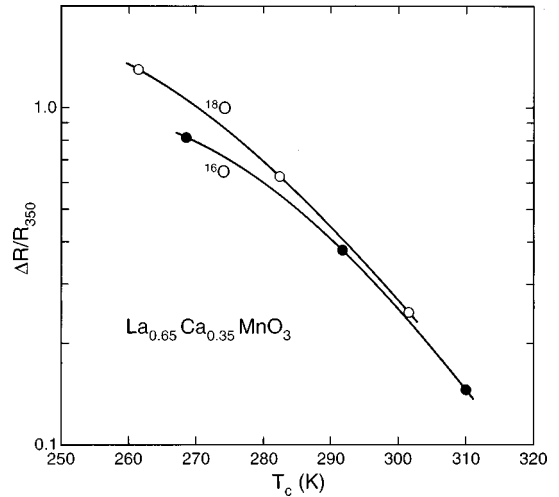


FIG. 3. The relative resistive peak height $[R(T_c) - R(350 \text{ K})] / R(350 \text{ K})$ as a function of Curie temperature T_c , $x_{\text{Ca}} = 35\%$.

hopping geometry. With $a = 3.9 \text{ \AA}$, we obtain $g_d \nu_o = 1.61 \times 10^{13} \text{ Hz}$ for ^{16}O and $g_d \nu_o = 1.86 \times 10^{13} \text{ Hz}$ for ^{18}O .

Since the Curie temperature T_c is very close to the resistivity maximum, one can use these data to obtain resistively determined isotope effects for fields up to 4 T. In Fig. 1 we have indicated the position of the resistive maximum in 0 T, it is seen to be close to the onset of the magnetic transition, for both the ^{16}O and ^{18}O samples. The resistively determined shift is, therefore, very close to the magnetic shift. For higher fields the resistive maximum moves rapidly to higher temperatures, and broadens, Fig. 2. In spite of the broadening, we can estimate the isotopic temperature shift within about $\pm 1.5 \text{ K}$ (0 T) and $\pm 2.5 \text{ K}$ (4 T). This leads to uncertainties in α_O of about ± 0.05 . We find at 0 T a $(\Delta T_c)_{\text{res}} = 7.1 \text{ K}$, $\alpha_O = 0.23$, at 2 T a $(\Delta T_c)_{\text{res}} = 9.40$, $\alpha_O = 0.28$ and at 4 T a $(\Delta T_c)_{\text{res}} = 8.5 \text{ K}$, $\alpha_O = 0.24$. In a field of 4 T the magnetization at the resistive maximum is about 20% of the saturation value at low temperatures. We see, therefore, no dependence of the isotope exponent on field up to 4 T, within experimental error.

Isotopic substitution of ^{18}O does not only reduce T_c , but it also sharpens the resistive peak. We describe the peak sharpness by comparing it to the resistivity at 350 K, $\Delta R / R_{350} = [R(T_c) - R_{350}] / R_{350}$. We find that this ratio at given field is increased by 60% in the ^{18}O substituted samples, independent of field up to 4 T. As a function of transition temperature, $\Delta R / R_{350}$ is approximately a universal curve, Fig. 3. The effect of isotopic substitution is, therefore, qualitatively similar to that of an applied field, with the smaller mass (^{16}O) corresponding to a larger field. Similar behavior was also observed in the pressure effect, where larger pressure increases T_c and broadens the resistivity peak.²¹

Raman scattering measurements identified two strong oxygen related lines near 225 and 430 cm^{-1} . The isotopic frequency shift (at 0 K) of the 225 cm^{-1} line is $8 \pm 1 \text{ cm}^{-1} = 3.5\%$, and of the 430 cm^{-1} line it is $21 \pm 1 \text{ cm}^{-1} = 4.8\%$. For an ^{18}O concentration of 82% we would expect a (harmonic) shift of 5.0%, which is close to the 430 cm^{-1} line shift. The lower frequency line is apparently hybridized with heavier ion (Mn) vibrations. Both lines

TABLE I. Oxygen-isotope dependence of the paramagnetic to ferromagnetic conducting transition of $\text{La}_{1-x}\text{Ca}_x\text{MnO}_3$.

x (%)	$T_c(^{16}\text{O})$ (K)	$T_c(^{18}\text{O})$ (K)	ΔT_c (K)	α_O	$\langle r_A \rangle$	t
20	222.7	202.0	20.7	0.83	1.356	0.9638
20 ^a	200.8	192.8	8.0	0.34	1.356	0.9638
20 ^b	243.0	229.5	13.5	0.48	1.356	0.9638
22	259.5	248.6	10.9	0.36	1.356	0.9647
25	266.8	257.0	9.8	0.32	1.355	0.9662
30	272.0	262.4	9.6	0.30	1.354	0.9686
35	270.7	261.7	9.0	0.29	1.353	0.9710
40	271.3	265.0	6.3	0.20	1.352	0.9735
41	274.0	266.0	8.0	0.25	1.352	0.9740
42	257.3	251.6	5.7	0.19	1.352	0.9744
43	260.3	255.9	4.4	0.14	1.351	0.9749

^aAfter 24 h in argon at 950 °C.

^b24 h in O_2 (1 atm) at 1175 °C, oven cooled.

show considerable hardening (and sharpening) with falling temperature below T_c , 3.5 to 4.5% for the low frequency line, and 1.3 to 1.4% for the high frequency line. A similar hardening of about 3% was also observed in infrared active lines at 330 and 550 cm^{-1} by Kim *et al.*²² The Raman data will be more fully discussed in a separate paper.

In order to establish the dependence of the isotope effect on Ca concentration over the whole ferromagnetic conducting range, we prepared powder samples at various other concentrations. For these samples only the isotopic shift at low fields was determined by magnetization measurements in 50 G. For high Ca concentrations, $x \geq 42\%$, we observe two transitions, at high temperatures the transition to the ferromagnetic conducting phase and at somewhat lower temperatures to the charge-ordered insulating phase. Large isotope shifts are seen in the charge-ordering transition, they will be reported in a separate paper.²³ In contrast to this, the isotope shift of the ferromagnetic T_c is quite small, with α_O near 0.1 in this range. At the low Ca concentration of 20% we find a very large isotope exponent of $\alpha_O = 0.83$, in excellent agreement with the data of Zhao *et al.*¹⁷ For a slightly larger x of 22% Ca, α_O drops to about 0.38 and then continues to fall with increasing Ca concentration. These data are given in Table I, and shown in Fig. 4, as function of Ca concentration and tolerance factor (see below).

The results at the calcium concentration of 20% are clearly different from the trend seen at larger concentrations. At 20% Ca, one lies at the border of the conducting and insulating-ferromagnetic phases. At this concentration, the magnetic properties are very sensitive to the total oxygen content.^{24,25} In particular, annealing at the relatively low temperature of 950 °C in 1 atm of O_2 can lead to excess oxygen content above 3.0. In order to check this, we heated this sample pair in pure argon at 950 °C for 24 h. We found that the magnetic transitions sharpened, the $T_c(^{16}\text{O})$ moved from 222.7 to 200.8 K, and α_O was reduced to 0.34. This latter value is in line with those for larger calcium concentrations. A second identical argon treatment did not change the data.

A second comparison pair with 20% Ca was then prepared, annealed for 24 h at 1175 °C and oven cooled. This

annealing temperature should lead to nearly $\text{O}_{3.0}$ content.²⁵ We achieved an ^{18}O content of 96% (by weight), and observed an isotope exponent of 0.48. The transition temperatures had increased and the transitions are sharp. We suspect, therefore, that the large isotope exponents between 0.8 and 0.9 in 20% Ca samples refer to samples with oxygen excess. From a study of the end member $\text{LaMnO}_{3+\delta}$ it was found²⁶ that an oxygen excess is accommodated in the structure through vacancies at the La and Mn sites. This will lead to locally strongly distorted structures. For x larger than 0.20, the oxygen content is close to the stoichiometric value 3.0, see Ref. 3. This is also evident from our results at $x = 0.35$, where T_c and α_O are largely independent of heat treatment.

Discussion of the properties of perovskite manganites are often carried out in terms of effective radii, in the form of the tolerance factor:²⁷

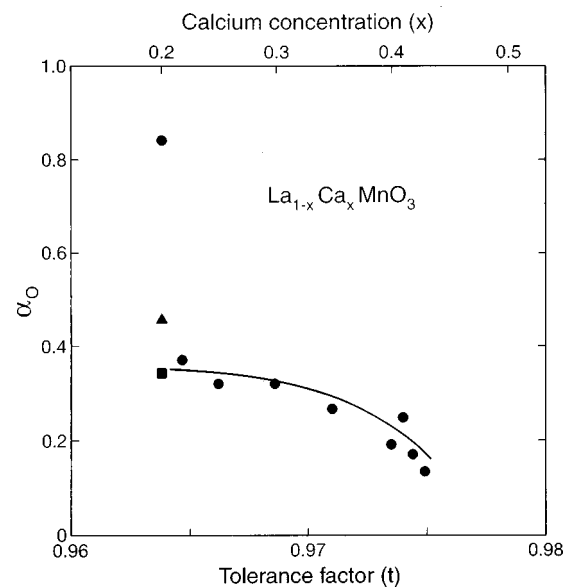


FIG. 4. The oxygen-isotope exponent α_O for $\text{La}_{1-x}\text{Ca}_x\text{MnO}_3$ as function of tolerance factor t , lower scale, and calcium concentration x , upper scale. Black dots, gas exchanged at 950 °C. Black square, heated in argon at 950 °C (24 h). Black triangle, heated in 1 atm O_2 at 1175 °C (24 h), oven cooled.

$$t = \frac{1}{\sqrt{2}} (\langle r_A \rangle + r_O) / (\langle r_B \rangle + r_O), \quad (3)$$

where $\langle r_A \rangle$ is the average radius of the A site ion (La or Ca) and $\langle r_B \rangle$ of the B site ion (Mn) in the perovskite structure. It was shown, e.g., that both the resistivity, transition temperature, and pressure effect can be described as a simple function of $\langle r_A \rangle$ (Refs. 21, 28, and 29) for given hole concentration. The tolerance factor relates to deviations from the ideal perovskite structure, which is obtained at $t=1$. The structure is also stable for $t < 1$ to about $t=0.75$. In this case the MnO_6 polyhedra adjust themselves to a too small A atom by rotation and tilting. This, in turn, leads to deviations of the Mn-O-Mn angle from 180° , reducing the double exchange interaction. The relation between tolerance factor and bond angle in perovskites was given by Sasaki *et al.*³⁰ The tolerance factor t is calculated by using average values for r_A and r_B for the case of a mixture of La and Ca in the A site and Mn^{3+} and Mn^{4+} in the B site. We use the ionic radii of Shanon,³¹ in 12-fold coordination for the A atoms, and in 6-fold coordination for the B atom. These values are $r(\text{La}^{3+})=1.36 \text{ \AA}$, $r(\text{Ca}^{2+})=1.34 \text{ \AA}$, $r(\text{Mn}^{3+})=0.645 \text{ \AA}$, $r(\text{Mn}^{4+})=0.53 \text{ \AA}$. For r_O we use 1.40 \AA . For an oxygen formula content of 3.0, one finds the Mn^{4+} concentration is equal to x . We have calculated the tolerance factor over the range of our data from $x=20$ to 43% under the assumption that x equals the Mn^{4+} concentration. With increasing Ca concentration, the average A site ion size decreases by 0.34% and the average B site ion size decreases by 4.44%. Both effects result in an increase of the tolerance factor by 1.15%. The major effect on t , and therefore, the Mn-O-Mn angle, is the decrease in the Mn-O_6 polyhedra size; compared to this the change in A site ion size is small.

The calculated average A site ion size $\langle r_A \rangle$, and the tolerance factor, are given in Table I. It should be remarked that different authors have used different ionic radii, so that direct

comparisons are not always possible. The relative dependence of $\langle r_A \rangle$ and t on Ca concentration is, however, not much affected by this. The isotope exponent α_O as function of the tolerance factor is shown in Fig. 4.

We find then that the isotope exponent α_O over the Ca concentration that leads to the ferromagnetic metallic phase, decreases from a relative high value near 0.36, to low values near 0.1 as the Ca concentration, and the tolerance factor t increase. The average A site ion size decreases in this range, the dependence on Ca concentration is, therefore, opposite to that seen in Ref. 17. In that work, however, no results inside the ferromagnetic conducting range were given. An isotopic shift of 9.7 K in the thermal expansion peak of $\text{La}_{0.67}\text{Ca}_{0.33}\text{Mn}_{0.3}$ was seen by Zhao *et al.*³² in agreement with our work.

The observed isotope exponents show the strong lattice or phonon dependence of the ferromagnetic transition. The dependence on tolerance factor points towards an influence on the double exchange mechanism. The tight-binding bandwidth is given by³³

$$W = \text{const } \lambda \cos \phi \left\langle \cos \left(\frac{\Theta_{ij}}{2} \right) \right\rangle, \quad (4)$$

where λ is the overlap intergral, ϕ the Mn-O-Mn bond angle, and Θ_{ij} the angle between two Mn spins. Different experimental probes affect different terms in this expression, e.g., Θ_{ij} is affected by magnetic fields and ϕ and λ by pressure. The independence of α_O on field (at least at 35% Ca) suggest that isotopic substitution affects ϕ and possibly λ . It is, therefore, not unexpected that the pressure dependence also decreases drastically between 20 and 40% Ca.²¹

We benefited from discussions with W. E. Pickett, S. W. Cheong, P. B. Littlewood, J. B. Goodenough, D. Emin, and A. Bussmann-Holder. This research was supported by grants from the Natural Sciences and Engineering Research Council of Canada.

¹G. H. Jonker and J. H. van Santen, *Physica (Amsterdam)* **16**, 337 (1950).

²E. Wollan and W. C. Koehler, *Phys. Rev.* **100**, 545 (1955).

³P. Schiffer *et al.*, *Phys. Rev. Lett.* **75**, 3336 (1995).

⁴C. H. Cheng and S. W. Cheong, *Phys. Rev. Lett.* **76**, 4042 (1996).

⁵J. Volger, *Physica (Amsterdam)* **20**, 49 (1954).

⁶S. Jin *et al.*, *Science* **264**, 413 (1994).

⁷C. Zener, *Phys. Rev.* **82**, 403 (1951).

⁸J. Goodenough, *Phys. Rev.* **100**, 564 (1955).

⁹P. W. Anderson and H. Hasegawa, *Phys. Rev.* **100**, 675 (1955).

¹⁰A. J. Millis *et al.*, *Phys. Rev. Lett.* **74**, 5144 (1995).

¹¹A. J. Millis *et al.*, *Phys. Rev. B* **54**, 5389 (1996); **54**, 5405 (1996).

¹²H. Röder *et al.*, *Phys. Rev. Lett.* **76**, 1356 (1996).

¹³M. Jaime *et al.*, *Phys. Rev. B* **54**, 11 914 (1996).

¹⁴H. Y. Hwang *et al.*, *Phys. Rev. Lett.* **75**, 914 (1995).

¹⁵R. H. Heffner *et al.*, *Phys. Rev. Lett.* **77**, 1869 (1996).

¹⁶A. Shengalaya *et al.*, *Phys. Rev. Lett.* **77**, 5296 (1996).

¹⁷Guo-meng Zhao *et al.*, *Nature (London)* **381**, 676 (1996).

¹⁸J. P. Franck *et al.*, *Physica C* **172**, 90 (1990).

¹⁹D. Emin and T. Holstein, *Ann. Phys. (N.Y.)* **53**, 439 (1969).

²⁰M. Jaime *et al.*, *Phys. Rev. Lett.* **78**, 951 (1997).

²¹See, e.g., J. J. Neumeier *et al.*, *Phys. Rev. B* **52**, R7006 (1995).

²²K. H. Kim *et al.*, *Phys. Rev. Lett.* **77**, 1877 (1996).

²³I. Isaac and J. P. Franck, *Phys. Rev. B* **57**, R5602 (1998).

²⁴S. Tamura, *Phys. Lett.* **78A**, 401 (1980).

²⁵S. Tamura and A. Yamamoto, *J. Mater. Sci.* **15**, 2120 (1980).

²⁶J. A. M. Van Roosmalen *et al.*, *J. Solid State Chem.* **110**, 100 (1994).

²⁷H. D. Megaw, *Trans. Faraday Soc.* **A42**, 224 (1946).

²⁸H. Y. Hwang *et al.*, *Phys. Rev. B* **52**, 15 046 (1995).

²⁹J. Fontcuberta *et al.*, *Phys. Rev. Lett.* **76**, 1122 (1996).

³⁰S. Sasaki *et al.*, *Acta Crystallogr., Sect. C: Cryst. Struct. Commun.* **43**, 1668 (1987).

³¹R. D. Shanon, *Acta Crystallogr., Sect. A: Cryst. Phys., Diff., Theor. Gen. Crystallogr.* **32**, 751 (1976).

³²Guo-meng Zhao *et al.*, *Phys. Rev. Lett.* **78**, 955 (1997).

³³J. B. Goodenough, *J. Appl. Phys.* **81**, 5330 (1997).